

1 Article

2 

# Coupled electric and hydraulic control of a PRS

  
3 

# turbine in a real transport water network

4 **Marco Sinagra <sup>1,\*</sup>, Costanza Aricò<sup>1</sup>, Tullio Tucciarelli<sup>1</sup>, Pietro Amato<sup>2</sup> and Michele Fiorino<sup>3</sup>**5 <sup>1</sup> Dipartimento di Ingegneria, Università degli Studi di Palermo, viale delle Scienze, 90128, Palermo, Italy;  
6 marco.sinagra@unipa.it, costanza.arico@unipa.it, tullio.tucciarelli@unipa.it7 <sup>2</sup> WECONS company, via Agrigento n.67, 90141, Palermo, Italy;  
8 p.amato@wecons.it9 <sup>3</sup> Layer Electronics company, S.P. KM 5,3 C.da S. Cusumano, 91100 Erice (TP) - Italy;  
10 info@layer.it

11 \* Correspondence: marco.sinagra@unipa.it; Tel.: +39-091-238-96518

12

13 **Abstract:** Although many devices have recently been proposed for pressure regulation and energy  
14 harvesting in water distribution and transport networks, very few applications are still  
15 documented in the scientific literature. A new in-line Banki turbine with positive outflow pressure  
16 and a mobile regulating flap, named PRS, was installed and tested in a real water transport  
17 network for pressure and discharge regulation. The PRS turbine was directly connected to a 55 kW  
18 asynchronous generator with variable rotational velocity, coupled to an inverter. The start-up tests  
19 showed how automatic adjustment of the flap position and the impeller velocity variation are able  
20 to change the characteristic curve of the PRS according to the flow delivered by the water manager  
21 or to the pressure set-point assigned downstream or upstream of the system, still keeping good  
22 efficiency values in hydropower production.23 **Keywords:** Pressure control; Micro-hydropower; Energy recovery; Water distribution network;  
24 Banki turbine; Energy harvesting

25

26 

## 1. Introduction

27 Although many cities continue to use fossil fuels as their main energy source, the use of renewable  
28 energy sources [1] is becoming a key political solution to mitigate climate changes occurring in the  
29 world. In this context the economic and social value of water is due today not only to its domestic  
30 and agricultural use, but also to the potential energy embedded in its delivery to low-altitude urban  
31 areas [2,3]. Water distribution or transport networks have been traditionally designed to meet  
32 consumer demands, usually variable over time, at the outlet of the pipe network, while keeping the  
33 pressure within a given pressure range, to provide a high quality service level. Recently new design  
34 approaches have also been based on additional hydraulic parameters such as resilience [4]. In both  
35 cases, to control discharge and pressure in the water network, along the pipelines water managers  
36 very often install pressure reducing valves (PRV) and needle valves. PRVs are aimed to control  
37 pressure in the conduit for a given demand and needle valves are aimed to control discharge given  
38 fixed outlet pressure [5,8]. An alternative to the use of valves is the use of Pumps As Turbines (PATs)  
39 or small hydraulic turbines [9] to convert hydraulic energy into electricity as an alternative to  
40 dissipation.41 Nowadays many studies can be found in the literature about the use of turbines with free outlet  
42 discharge [10,14] or positive outlet pressure [15]. However, the use of these turbines is limited by

43 their high cost, compared to the gross power usually available in the pipelines. For these  
44 applications less expensive solutions are Crossflow mini-turbines [16] in the case of free outlet  
45 discharge and PATs [17,18] in the case of positive outlet pressure. The main drawback of PATs is  
46 given by the need to dissipate part of the available energy when the discharge or head jump values  
47 required by the water manager are different from the design ones, due to the absence of any  
48 hydraulic system to control the characteristic curve [17]. To maintain hydraulic control of the  
49 network, PATs [20,21] and Crossflows [22] are often coupled with electronic systems for regulation  
50 of impeller rotation velocity or with installation of PRV valves in series or parallel with the PAT [23].  
51 This type of solution is also applied for the recharge of electric vehicles in urban areas [24].  
52 An alternative, more efficient and also less expensive way to produce hydropower while keeping the  
53 hydraulic control of the network is given by a new Crossflow-type of turbine, named PRS and  
54 already proposed by the authors in previous numerical [25] and laboratory experimental studies  
55 [26]. PRS has the simplicity of Crossflow turbines, but is also equipped with a hydraulic regulation  
56 system which allows changes in the characteristic curve according to the specific discharge or to the  
57 head jump required by the water manager. In this paper the design, the installation in a Sicilian  
58 aqueduct and the start-up tests of a 55 kW PRS turbine, subject to discharge and pressure variations,  
59 are described and analyzed for the first time.

## 60 2. PRS turbine

61 The PRS turbine is a new in-line Crossflow type micro-turbine, with positive outflow pressure and a  
62 mobile regulation flap for hydraulic control of the characteristic curve, developed and tested by the  
63 authors at the hydraulic laboratory of the University of Palermo [25-27].

64 A PRS turbine has five main components (Fig. Figure 1): the convergent pipe, the nozzle, the  
65 mobile flap, the rotating impeller and the pressurized diffuser. The convergent pipe is aimed to  
66 accelerate the particles, transforming most of the potential pressure energy into kinetic energy, and  
67 the nozzle works as a/the distributor of the discharge entering the impeller through the inlet surface.  
68 The mobile flap varies the inlet surface in the impeller, in order to control the velocity of the inlet  
69 particle during any change in the discharge and to keep constant the ratio between the tangent  
70 velocity component of the particle and the impeller rotational velocity at the same inlet location. The  
71 impeller inlet and outlet surfaces are part of a cylinder, with generator lines parallel to the axis and  
72 laterally bounded by the two impeller disks. The two impeller disks form a single solid block with  
73 the blades, which are semi-circular and have a constant inner radius. Water flow goes through the  
74 blade channels twice, before leaving the impeller and entering the diffuser section. This part, which  
75 is missing in the original Crossflow turbine for zero-pressure outlet flow, is designed in order to  
76 minimize dissipation of the particle-specific energy along the path between the impeller and the  
77 outlet section of the turbine case. The PRS turbine can be set in the "passive" or "active" mode. In the  
78 former the device is used to set the piezometric level at any required value, lower than the inlet one,  
79 but even much greater than the ground elevation, while also being variable in time. In the "active"  
80 mode, the device is used to set the discharge at any required value by controlling the flap position  
81 and the pressure reduction occurring between the inlet and outlet pipe sections.

82

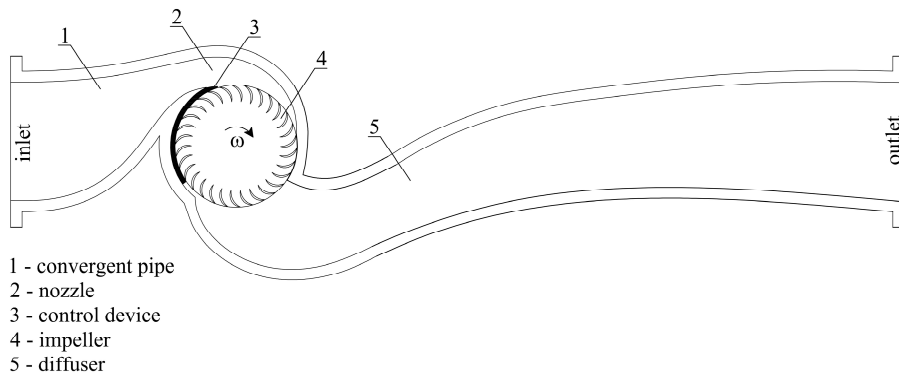


Figure 1. Vertical section of a PRS turbine.

83  
84  
85  
86  
87  
88  
89  
90

Turbine design has to satisfy three conditions assigned at the Best Efficiency Point (BEP) among the impeller diameter  $D$ , the rotational velocity  $\omega$ , the discharge  $Q$  and the net head  $\Delta H$  occurring between the inlet and the outlet pipes. The first equation is the energy conservation equation, which according to previous studies ([25]-[27]) is given by:

91  
92  
93  
94  
95  
96  
97  
98  
99  
100  
101  
102  
103

$$V = C_V \sqrt{2g \left( \Delta H - \xi \frac{\omega^2 D^2}{8g} \right)} \quad (1),$$

where  $V$  is the velocity norm at the impeller inlet surface,  $C_V = 0.98$ ,  $\xi = 2.1$  and  $g$  is the gravitational acceleration.

The second equation is the mass conservation equation, which provides:

$$Q = \frac{BD\lambda_{rmax} V \sin \alpha}{2} \quad (2),$$

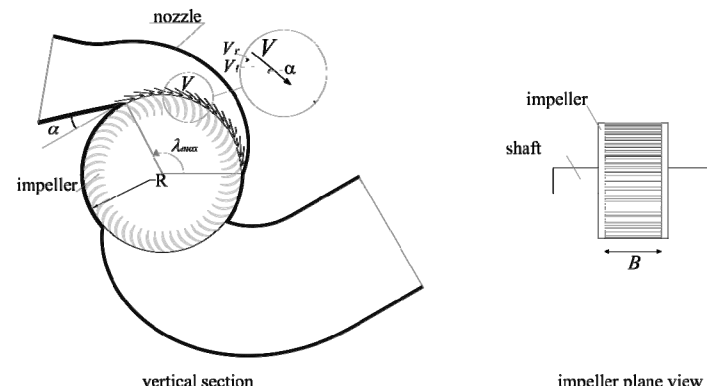
where  $B$  is the impeller width,  $\lambda_{rmax}$  is the maximum inlet angle, equal to  $110^\circ$ , and  $\alpha$  is the angle between the particle velocity and the tangent direction at the impeller inlet (Fig. Figure 2), approximately equal to  $15^\circ$ . The third equation is the optimality condition of the velocity ratio  $V_r$ , defined as the ratio between the tangent component of the inlet velocity and the impeller rotational velocity at the same inlet surface, that is:

$$V_r = \frac{DV \cos \alpha}{2\omega} \quad (3).$$

Sinagra et al. [25] showed that the maximum efficiency in PRS turbine is obtained assuming  $V_r = 1.7$ .

The diameter  $D$  and width  $B$  can be found by fixing in Eqs (1) and (3) the rotational velocity  $\omega$ , and by solving the system of Eqs. (1)-(3) in the unknowns  $V$ ,  $D$  and  $B$ . This is the commonest approach for the design of mini-hydroturbines, where the impeller is directly connected to the shaft of the asynchronous electric generator, which has a fixed rotational velocity.

111



112

113 **Figure 2.** Nozzle and impeller geometry of PRS turbine.114 **3. Electrical energy production and velocity regulation**

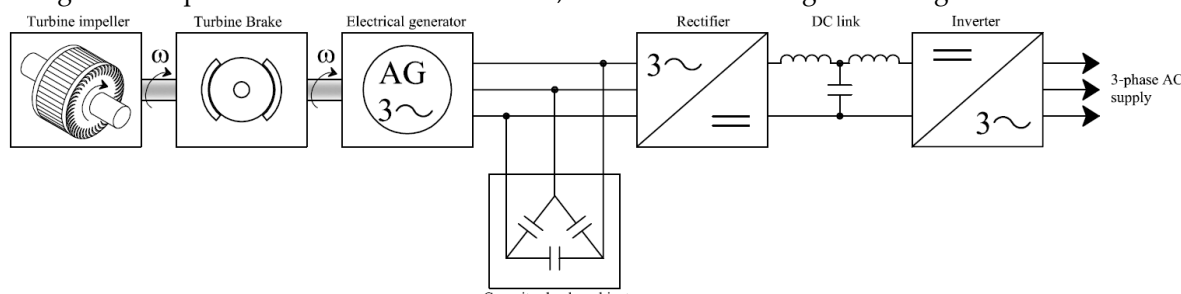
115 In small-scale hydroelectric plants, with power lower than 250 kW, the simplest way to convert  
 116 hydraulic power into electrical power is to couple an asynchronous three-phase generator to the  
 117 turbine impeller. In case (A), when the electric generator is directly connected to the AC grid, the  
 118 reactive power required by the electrical generator to properly operate is provided by the grid itself,  
 119 while in case (B), that of a stand-alone plant, the reactive power is provided by a local capacitor bank.  
 120 The choice of the asynchronous generator is motivated by its simplicity and robustness. However, in  
 121 both operation modes A and B, the rotational velocity of the electric generator is closely related to  
 122 the frequency  $f$  of the AC grid (grid-connected) or of the electrical equipment (stand-alone), which in  
 123 Europe is equal to 50 Hz, through the equation:

$$124 \quad \omega = \frac{60f}{2p} \quad (4),$$

125 where  $\omega$  is the rotational velocity in rotations per minute and  $p$  is the number of poles.

126 When the net head  $\Delta H$  changes along with the operating conditions of the hydraulic network,  
 127 equations (1) and (3) cannot be satisfied together with same diameter  $D$ , unless the impeller  
 128 rotational velocity  $\omega$  is changed. For this reason, the rotational velocity of the impeller is optimized  
 129 by means of an electric system. The electric regulation system consists of a rectifier and an inverter.  
 130 The task of the rectifier is to convert the alternating voltage supplied by the asynchronous  
 131 three-phase generator, working at variable voltage and frequency, into a continuous voltage for the  
 132 inverter power supply. The inverter adopted is a total-control IGBT bridge in configuration B6 (three  
 133 branches in parallel, each one with two IGBTs in series), which commutes the continuous voltage  
 134 supplied by the rectifier into a sinusoidal alternating voltage at 50Hz. The reactive power required  
 135 by the electrical generator is provided in the stand-alone case by a local capacitor banks cabinet with  
 136 automatic power control (Figure 3).

137 With this configuration, the optimal rotational velocity  $\omega$  of the impeller is automatically  
 138 attained in case B by regulating the voltage coming out of the inverter. Higher electric loads will lead  
 139 to higher power, but also to a reduction of the turbine rotational velocity, due to a torque resistance  
 140 increment. This implies that the system will shortly reach an equilibrium condition that will change,  
 141 along with the power delivered in the network, as a function of the given voltage.



142

143 **Figure 3.** Block diagram of a direct drive power conversion unit.

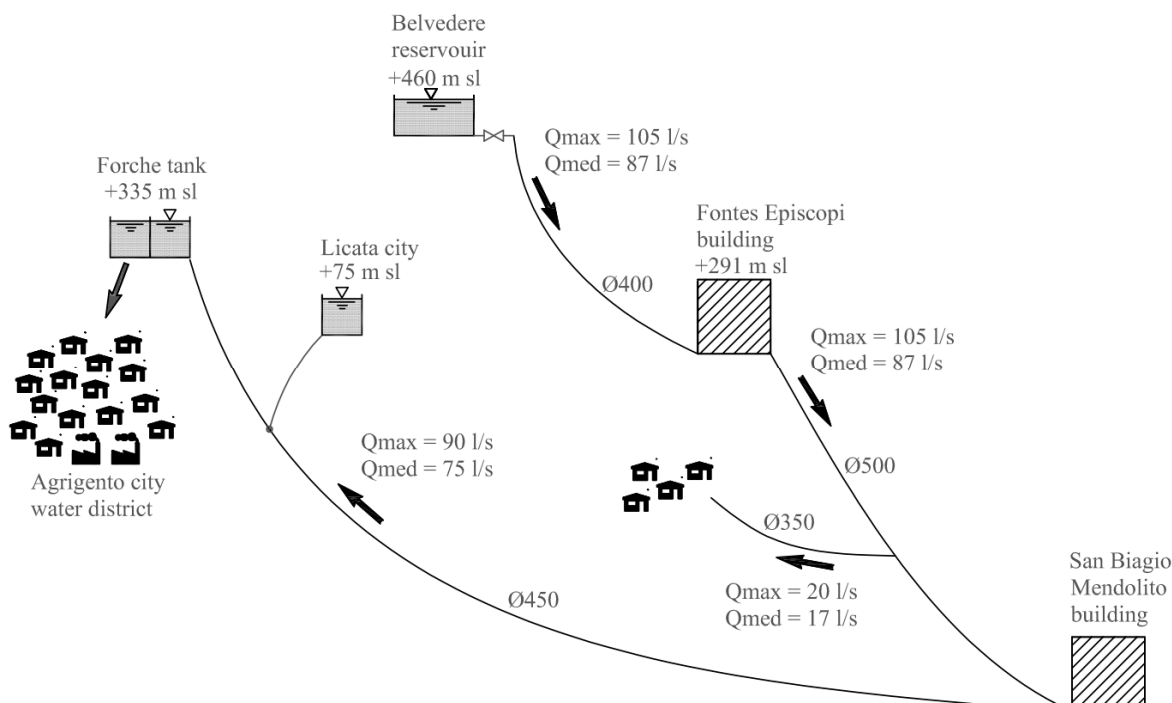
144 A similar scheme can be attained in case A, by disconnecting the capacitor banks cabinet and  
 145 regulating the current coming out of the inverter.

146 **4. Study case: Gela-Aragona aqueduct**

147 We investigated the design and management of a PRS turbine inline of an oversized water transport  
 148 network, subject to continuous discharge regulations due to the changing demand of water users.

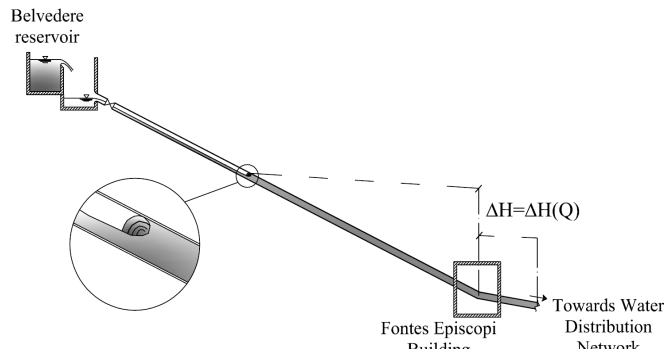
149 The water transport network, called the Gela-Aragona aqueduct, is part of the larger Water  
 150 Transport Network of Sicily (Italy). The Gela-Ragona aqueduct starts from an upper tank, called  
 151 "Belvedere" and located at an altitude of 460 m above sea level, supplying a lower tank named  
 152 "Forche", located 335 m above sea level. This tank supplies the water distribution network of the city  
 153 of Agrigento, as well as another tank located at an altitude of 75 m above sea level, serving the water  
 154 distribution network of the town of Licata. Along the pipeline there are two pressure maneuvering  
 155 buildings, called "Fontes Episcopi" and "San Biagio Mendolito", and between them there is a  
 156 derivation supplying a small urban center (Fig. Figure 4). The discharge from the "Belvedere"  
 157 reservoir changes in the range 70-100 l/s, and is regulated at present by a needle valve located  
 158 immediately downstream of the reservoir. Inside the cited discharge range the pressure measured at  
 159 the "Fontes Episcopi" building changes in the range 0.2 - 0.6 MPa. If the pressure measured at  
 160 "Fontes Episcopi" is above 0.5 MPa, the "Forche" tank is filled; otherwise the flow is conveyed  
 161 entirely to the Licata tank.

162



163  
 164 **Figure 4.** Scheme of the water transport network.  
 165

166 Inside the cited discharge range, the pipeline connecting the "Belvedere" reservoir to the  
 167 "Fontes Episcopi" building, which is 3.5 km long, is not completely full and the pressure drop  $\Delta H$  of  
 168 the free surface transition section inside the pipeline, with respect to the piezometric level at the  
 169 "Fontes Episcopi" building, is approximately proportional to the square of the discharge released  
 170 through the needle valve by the water manager (Fig. Figure 5).  
 171

172  
173  
174

**Figure 5.** Hydraulic regime inside the upstream pipeline without the PRS turbine.

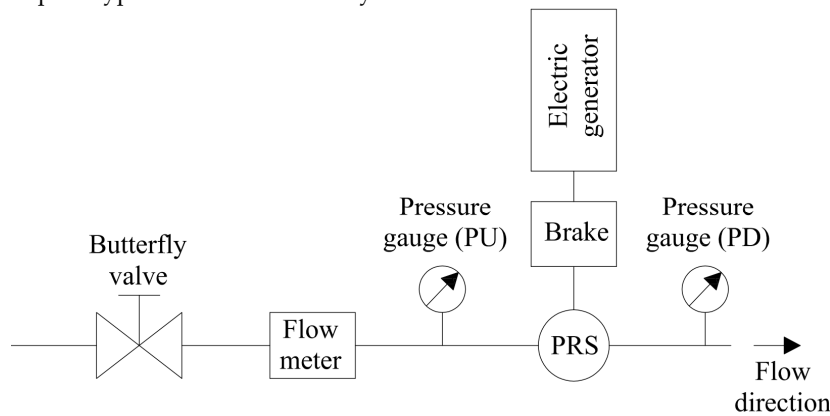
175 These operating conditions provide a hydraulic jump available for hydroelectric production  
176 between the surface transition and the "Belvedere" reservoir, which can be converted into electricity  
177 by a PRS turbine installed inside the Fontes Episcopi building at an altitude of 291 m above sea level.  
178 The maximum electricity production would occur in the case of a fully pressurized pipe, with head  
179 losses equal to 9.00 m in the case of a maximum flow rate. In order to guarantee the maximum flow  
180 rate when the maximum pressure occurs at Fontes Episcopi (0.6 MPa = 60m), the following values  
181 were assumed in Eqs. (1)-(3) for the design of parameters  $D$  and  $B$  in the condition of a fully opened  
182 flap:  $\Delta H = 100$  m and  $Q = 105$  l/s.

183 Assuming a rotational velocity  $\omega$  equal to 1510 rpm, the impeller diameter  $D$  and the width  $B$   
184 resulting from the procedure described in paragraph 2 are equal to 204 and 62 mm, respectively. The  
185 PRS casing is made of cast iron and the impeller, made of stainless steel, has 40 semicircular blades  
186 [28] connected to each other by a couple of circular plates fixed to the shaft, which rotates on two  
187 bearings. There is no internal shaft. The flap is made of stainless steel and is moved by a linear  
188 electrical actuator.

189 Small traditional hydroelectric plants are equipped with a synchronous by-pass to stop rotation  
190 of the impeller in the case of failure of the electric network. This is a pipe parallel to the impeller,  
191 equipped with an automatic valve, which opens to allow the entire flow to bypass the turbine when  
192 electricity is missing. In the Fontes Episcopi PRS plant an alternative solution was selected. Between  
193 the impeller shaft and the electric generator a negative electric-brake was installed. In the case of  
194 failure of the electrical grid or an emergency, the brake is activated instantaneously to stop rotation  
195 of the impeller rapidly. The total flow will continue to pass through the impeller, which will have  
196 zero speed. Observe that this solution guarantees water supply even in the absence of electricity  
197 production, without installing an automatic synchronous valve.

198 For electricity production, an asynchronous generator 4-pole IE2 efficiency class with 55 kW  
199 power was installed. The power electronics system described in paragraph 3, with a maximum  
200 electrical power of 60 kW, was connected to the electric generator. The power electronics was  
201 oversized compared to the generator power to ensure system security. In Figure 6 the PRS turbine  
202 prototype installed inside the Fontes Episcopi building is shown.

203 For monitoring hydraulic parameters, an electromagnetic flow meter and a digital pressure  
204 meter were installed upstream of the PRS prototype and a second digital pressure meter was  
205 installed downstream of the turbine to measure the net head of the turbine (Fig. Figure 7).  
206

207  
208**Figure 6.** PRS turbine prototype installed in the study case.209  
210**Figure 7.** Equipment installation scheme.

211

212  
213  
214  
215  
216  
217  
218

The PRS components of the pilot plant are automatically regulated by a PLC installed on the electrical panel dedicated to turbine management. If the device is used in “active” mode and the flow rate  $Q_{set}$  is set, the flap position is found by comparing the measure of the flow meter with its target value; if the device is used in “passive” mode, the flap position is found by comparing the pressure measured by the downstream or upstream pressure gauge with its pressure target value. In both cases, the impeller rotational velocity is optimized by maximizing the electrical power  $P_i$  coming out of the inverter, according to the  $Q_{set}$  or  $H_{set}$  values, calculated by the eq. 5:

219

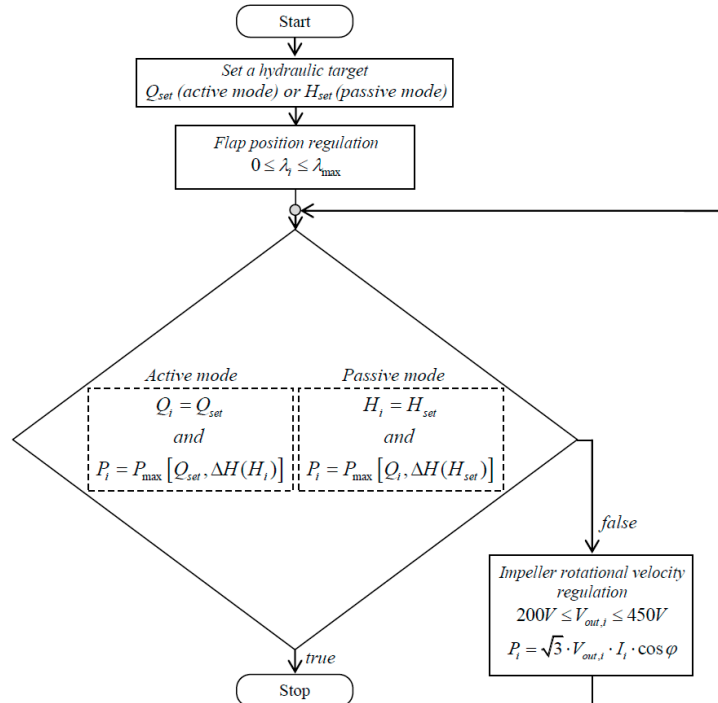
$$P_i = \sqrt{3} \cdot V_{out,i} \cdot I_i \cdot \cos \varphi \quad (5),$$

220  
221

where  $V_{out,i}$  and  $I_i$  are respectively the voltage and the current coming out of the inverter and  $\cos \varphi$  is the power factor.

222  
223

The control logic implemented in the PLC is represented by the flow chart in Figure 8.



224

Figure 8. Flow chart of PRS regulation.

225

226

227 The hydroelectric production performance of the plant is calculated by comparing in each time  
 228 the electrical output power from the inverter with the gross hydraulic power computed from the  
 229 flow and pressure measurements.

230

## 5. PRS turbine application results

231

232 During the start-up period, in order to guarantee the quality of water distribution and ensure the  
 233 safety of the pipeline, the water manager needs to guarantee the following operating conditions: 1) a  
 234 pressure in the range of 0.2-0.4 MPa downstream of the Fontes Episcopi building; 2) a pressure lower  
 235 than 1.0 MPa on the entire supply line; 3) discharge variable according to the given demand and in  
 236 any case lower than 75 l/s. Under these operation conditions, different from the turbine design  
 237 values, the PRS start-up tests were carried out.

238

239 In the following sections, the hydraulic and power variables recorded during the start-up tests  
 240 on the PRS plant installed at the Fontes Episcopi building are shown. Due to the long time required  
 241 by bureaucracy for connection to the Italian national electric grid and electricity trading, the  
 242 electrical power produced by the plant during the 2 days of the start-up tests was temporarily  
 243 dissipated through electrical resistances.

244

245 During the start-up period, the device was set in passive mode, with the discharge imposed by  
 246 the water manager through the needle valve and shown in Figs. Figure 9 and Figure 10. Observe that,  
 247 with the given discharge, free surface conditions always occur inside the upper part of the pipeline.  
 248 The pressure immediately upstream of the PRS was set according to the manager's request, given  
 249 the downstream pressure curve plotted in the same figures. On the first day of testing the maximum  
 250 upstream pressure was set at 0.8 MPa; on the second day of testing it was set at 1.0 MPa. The time  
 series of the hydraulic data recorded during the testing period are all shown in Figs. Figure 9  
 and Figure 10.

250

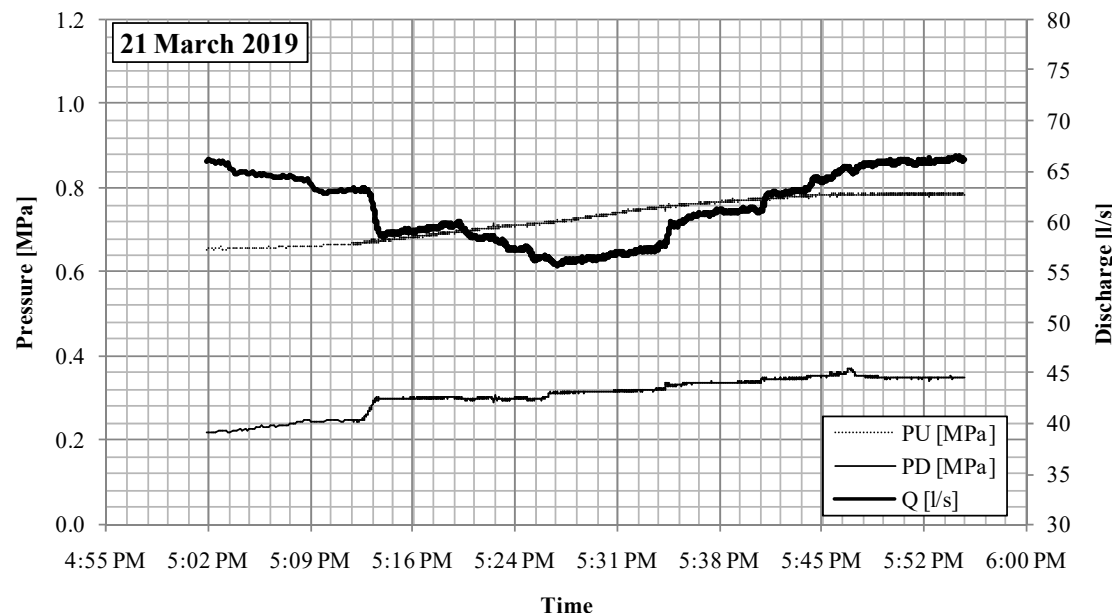
251  
252  
253

Figure 9. Discharge and pressure in the manometers showed in Figure 7.

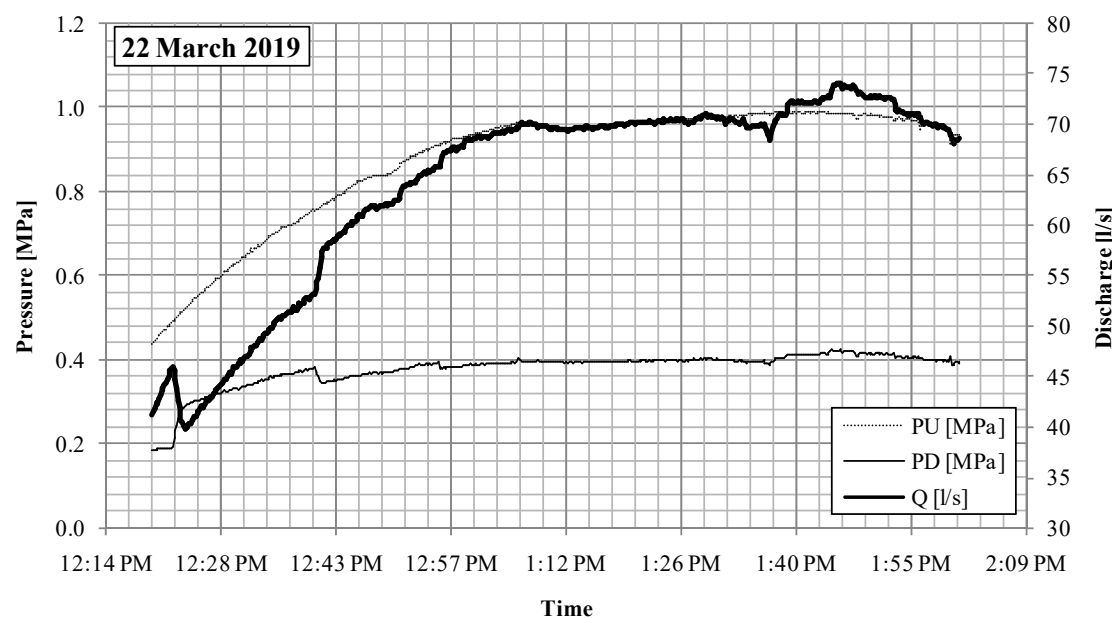
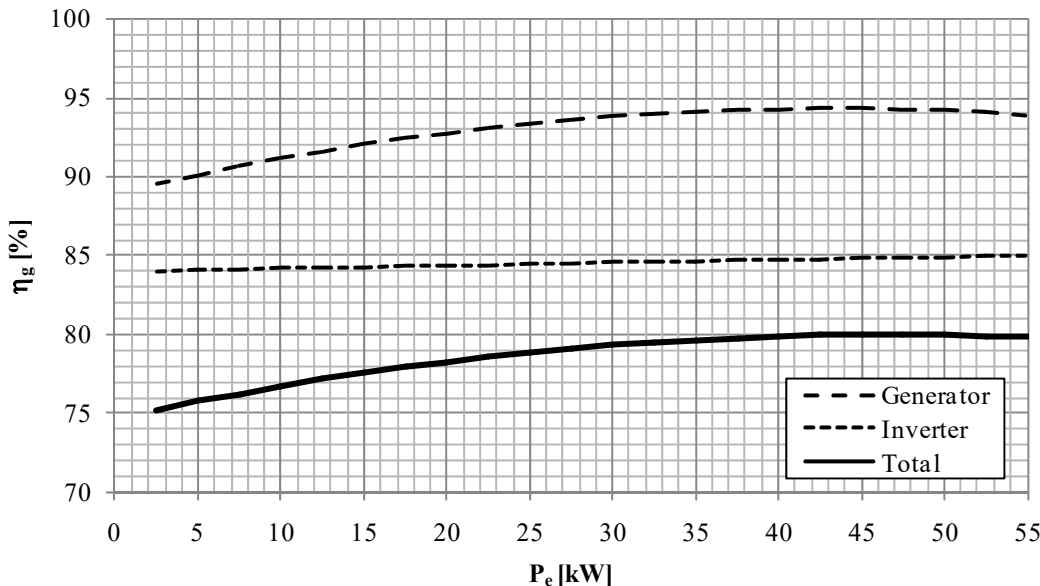
254  
255  
256

Figure 10. Discharge and pressure in the manometers showed in Figure 7.

257  
258  
259  
260  
261  
262  
263

In order to evaluate the global performance of the PRS and the hydroelectric plant, voltage and current measurements were made at the input and output of the inverter, to get the electrical power along the test time. Knowledge of the generator characteristic curve made it possible to determine the efficiency of the asynchronous generator as a function of the power supplied by the generator itself. The inverter's efficiency was estimated by comparing its input and the output power. The electrical efficiencies are shown in Figure 11. The graph shows that the inverter has lower efficiency than the electric generator, but that it is constant with respect to the supplied power.



264

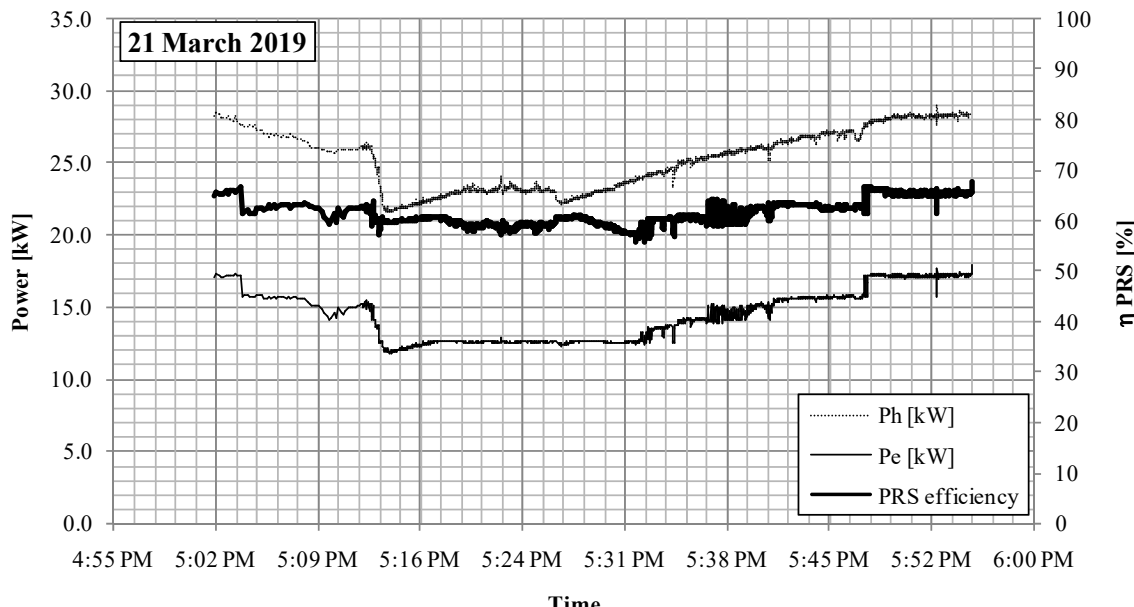
265

**Figure 11.** Electrical efficiencies.

266

267

The hydraulic efficiency of the PRS was computed as the ratio between the output electric power of the generator and the available gross hydraulic power, multiplied by the total electrical efficiency. The tests carried out show an average hydraulic efficiency of 61% on the first day and 55% on the second day of operation. The hydraulic efficiency of the PRS versus time is shown in Figs. Figure 12 and Figure 13.

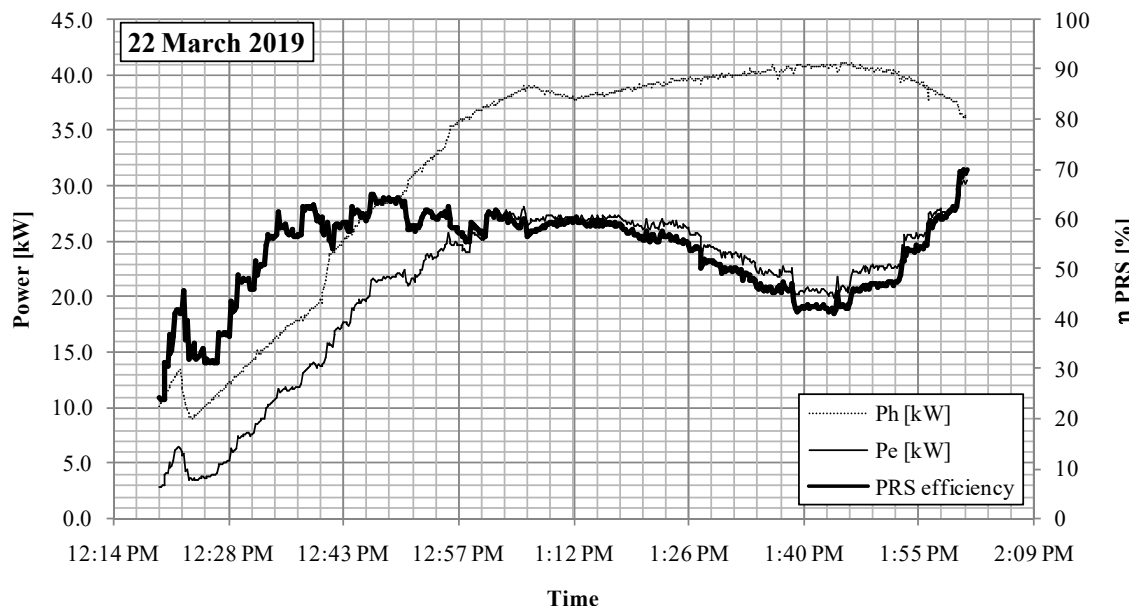


272

273

**Figure 12.** Hydraulic power, electrical power and PRS efficiency.

274



275  
276 **Figure 13.** Hydraulic power, electrical power and PRS efficiency.  
277

278 Some electrical disconnections of the generator were carried out during the start-up period, in  
279 order to validate the effect of brake action on the water supply and on the pipeline, for different  
280 discharge and pressure values. The tests confirmed the absence of overpressure in the pipeline  
281 generated by the instantaneous stop of the impeller and validated the 30% increment of the  
282 maximum discharge, as already numerically predicted by previous studies [25].

283 **6. Conclusions**

284 A new Banki-type turbine with positive outlet pressure, called PRS, was installed in a real water  
285 transport network for pressure regulation. The PRS is equipped with an internal flap for discharge  
286 or pressure regulation and an inverter for the impeller rotational velocity regulation. Start-up tests  
287 showed that the PRS could be efficiently used in water distribution networks for regulation of flow  
288 rate, as an alternative to needle valves, or for regulation of the downstream/upstream head, as an  
289 alternative to PRV valves. The tests also showed that the PRS is able automatically to adjust the  
290 position of its flap and optimize power production by rotational velocity regulation, according to the  
291 pressure set-point required by the water manager and the instantaneous discharge. Simulation of  
292 interruption of the electrical network also showed that the PRS braking system is able quickly to  
293 interrupt impeller rotation, without generating overpressures on the water network. The transition  
294 of the maximum flow through the stopped impeller provides a net head which is equal to the net  
295 head occurring at the optimal rotating velocity divided by 1.71, as already predicted in a previous  
296 study.

297 The hydraulic constraints imposed by the water manager during the start-up period did not  
298 allow use of the turbine according to the design conditions, but this is unfortunately the most  
299 common situation. In spite of that, the PRS mean efficiency, equal to 53% on the first testing day and  
300 61% on the second testing day, coupled with a total electrical efficiency of the order of 80%, still leads  
301 to a significant amount of energy and a corresponding gain for the water manager. The cost of  
302 installing the PRS is certainly superior to the installation of a simple dissipation device, but the  
303 significant electricity production that can be obtained from the PRS guarantees a financial benefit  
304 that is significantly higher than the installation costs in the case study.

305  
306 **Author Contributions:** All authors contributed to the development of this manuscript. Marco Sinagra,  
307 Costanza Aricò and Tullio Tucciarelli designed and supervised the hydraulic tests. Pietro Amato designed the  
308 PRS turbine and supervised the mechanical components. Michele Fiorino designed electrical control systems  
309 and supervised the electrical tests.

310 **Funding:** The experimental plant was funded by "Pressure Management System (PMS) project, grant number  
311 no. F/050304/01-03/X32 - Ministero dello Sviluppo Economico D.M. 1 Giugno 2016 Horizon 2020 – PON  
312 2014/2020".

313 **Acknowledgments:** We thank the BitControl srl, Layer Electronics srl and Vettorello srl companies, partners in  
314 the PMS project, for authorization of scientific use of the experimental results.

315 **Conflicts of Interest:** The authors declare no conflict of interest.

## 316 References

- 317 1. Perea-Moreno M.A.; Hernandez-Escobedo Q.; Perea-Moreno A.J. Renewable Energy in Urban Areas:  
318 Worldwide 2018, *Energies* **2018**, *11*, 577.
- 319 2. Dai J.; Wu S.; Han G.; Weinberg J.; Xie X.; Wu X.; Song X.; Jia B.; Xue W.; Yang Q.; Water-energy nexus: A  
320 review of methods and tools for macro-assessment, *Applied Energy* **2018**, *210*, 393–408.
- 321 3. Oikonomou K.; Parvania M. Optimal Coordination of Water Distribution Energy Flexibility With Power  
322 Systems Operation, *IEEE Transactions on Smart Grid* **2019**, *10*, *1*, 1101–1110.
- 323 4. Baños R.; Reca J.; Martínez J.; Gil C.; Márquez A.L. Resilience Indexes for Water Distribution Network  
324 Design: A Performance Analysis Under Demand Uncertainty. *Water Resources Management* **2011**, *25*,  
325 2351–2366.
- 326 5. Lotfizadeh H.R.; Barza H.; Abdevalipour M. Controlling the Water Pressure in the Pressure Control.  
327 *World Applied Sciences Journal* **2012**, *18* (8): 1088–1094.
- 328 6. Nazif S.; Karamouz M.; Tabesh M.; Moridi A. Pressure Management Model for Urban Water Distribution  
329 Networks. *Water Resour Manage* **2010**, *24*, 437–458.
- 330 7. Prescott S.; Ulanicki B. Improved Control of Pressure Reducing Valves in Water Distribution Networks. *J.*  
331 *Hydraul Eng* **2008**, *134*(1), 56–65.
- 332 8. Araujo L.; Ramos H.; Coelho S. Pressure control for leakage minimization in water distribution systems  
333 management. *Water Resources Management* **2006**, *20*(1), 133–149.
- 334 9. Carravetta A.; Fecarotta O.; Sinagra M.; Tucciarelli T. Cost-Benefit Analysis for Hydropower Production in  
335 Water Distribution Networks by a Pump as Turbine. *J. Water Resour. Plann. Manage.*, **2014**,  
336 10.1061/(ASCE)WR.1943-5452.0000384, 04014002.
- 337 10. Sammartano V.; Morreale G.; Sinagra M.; Tucciarelli T. Numerical and experimental investigation of a  
338 cross-flow water turbine. *Journal of Hydraulic Research*, **2016**, *55*:5, pages 686–694.
- 339 11. Coelho B., Andrade-Campos A., Energy Recovery in Water Networks: Numerical Decision Support Tool  
340 for Optimal Site and Selection of Micro Turbines, *Journal of Water Resources Planning and Management*  
341 **2018**, Vol. 144, Issue 3 (March 2018).
- 342 12. Khosrowpanah, S., Albertson, M., Fiuzat, A. Historical overview of Cross-Flow turbine. *Int Water Power  
343 Dam Constr.* **1984**, 38–43.
- 344 13. Sammartano, V., Aricò, C., Sinagra, M., Tucciarelli, T. Cross-Flow Turbine Design for Energy Production  
345 and Discharge Regulation. *J. Hydraul. Eng.* **2014**, 10.1061/(ASCE)HY.1943-7900.0000977, 04014083.
- 346 14. Sinagra, M., Sammartano, V., Aricò, C., Collura, A. Experimental and Numerical Analysis of a Cross-Flow  
347 Turbine. *J. Hydraul. Eng.* **2015**, 10.1061/(ASCE)HY.1943-7900.0001061, 04015040
- 348 15. Chen J.; Yang H.X.; Liu C.P.; Lau C.H.; Lo M. A novel vertical axis water turbine for power generation  
349 from water pipelines. *Energy* **2013**, *54*, 184–193
- 350 16. Sinagra M.; Sammartano V.; Aricò C.; Collura A. Experimental and Numerical Analysis of a Cross-Flow  
351 Turbine. *Journal of Hydraulic Engineering*, **2016**, *142* - 1 (January 2016).
- 352 17. Carravetta A.; Del Giudice G.; Fecarotta O.; Ramos H. Pump as Turbine (PAT) Design in Water  
353 Distribution Network by System Effectiveness. *Water*, **2013**, *5*(3), 1211–1225.
- 354 18. Yang S.; Derakhshan S.; Kong F. Theoretical, numerical and experimental prediction of pump as turbine  
355 performance. *Renewable Energy*, **2012**, 507–513
- 356 19. Carravetta A.; Del Giudice G.; Fecarotta O.; Ramos H. Energy Production in Water Distribution Networks:  
357 A PAT Design Strategy. *Water Resources Management*, **2012**, *26*, *13*, 3947–3959.
- 358 20. Carravetta A.; Del Giudice G.; Fecarotta O.; Ramos H.M. PAT Design Strategy for Energy Recovery in  
359 Water Distribution Networks by Electrical Regulation. *Energies*, **2013**, *6*(1), 411–424.

360 21. Fontana N.; Giugni M.; Glielmo L.; Marini G.; Zollo R. Hydraulic and Electric Regulation of a Prototype for  
361 Real-Time Control of Pressure and Hydropower Generation in a Water Distribution Network. *Journal of  
362 Water Resources Planning and Management*, **2018**, 144 (11).

363 22. Sammartano V.; Filianoti P.; Sinagra M.; Tucciarelli T.; Scelba G.; Morreale G. Coupled hydraulic and  
364 electronic regulation of cross-flow turbines in hydraulic plants. *Journal of Hydraulic Engineering*, **2017**,  
365 143 (1), art. no. 04016071.

366 23. Fecarotta O.; Aricò C.; Carravetta A.; Martino R.; Ramos H. M. Hydropower Potential in Water  
367 Distribution Networks: Pressure Control by PATs, *Water Resources Management*, **2015**, 29, 3, 699–714.

368 24. Balacco, G., Binetti, M., Caporaletti, V. et al. *Int J Energy Environ Eng*, **2018**, 9: 435

369 25. Sinagra M., Sammartano V., Morreale, G., Tucciarelli T. A new device for pressure control and energy  
370 recovery in water distribution networks. *Water*, **2017**, 9 (5).

371 26. Sammartano V.; Sinagra M.; Filianoti P.; Tucciarelli T. A Banki–Michell turbine for in-line water supply  
372 systems, *Journal of Hydraulic Research*, **2017**, 55(5), 686-694.

373 27. Sinagra M.; Aricò C.; Tucciarelli T.; Morreale G. Experimental and numerical analysis of a backpressure  
374 Banki inline turbine for pressure regulation and energy production. *Renewable energy*. Under review.

375 28. Sammartano, V., Aricò, C., Carravetta, A., Fecarotta, O., & Tucciarelli, T. Banki-Michell optimal design by  
376 computational fluid dynamics testing and hydrodynamic analysis. *Energies*, **2013**, 6(5), 2362–2385.